Numerical Analyses for Two-Phase Flow in a Vertical Cylinder

Kusu, Sunao
Interdisciplinary Graduate School of Engineering Sciences Kyushu University

Kuwagi, Kenya
Interdisciplinary Graduate School of Engineering Sciences Kyushu University

Ozoe, Hiroyuki
Institute of Advanced Material Study Kyushu University

https://doi.org/10.15017/7879

出版情報：九州大学機能物質科学研究所報告. 11 (2), pp.141-145, 1997-12-15. Institute of Advanced Material Study Kyushu University
バージョン：
権利関係：

Numerical Analyses for Two-Phase Flow in a Vertical Cylinder

Sunao KUSU*, Kenya KUWAGI* and Hiroyuki OZOE

Two-dimensional computational model for two-phase flow in a vertical cylindrical tank was derived and computed successfully. The height of a cylinder is 8 cm and the diameter of a cylinder is 16 cm. Air was injected through a glass filter located at a bottom center of a water tank. Computational model is based on a dispersed model after Kataoka and Tomiyama. Effect of computational grid sizes and the boundary condition at a top surface of water are studied. Computed results are compared with flow visualized experimental results and confirmed that the rigid surface condition is better than free slip condition.

Introduction

The two-phase flow consisting of gas and liquid is commonly encountered in many industrial processes and its transport phenomena is quite important to be clarified for a design of related chemical plant such as bubble columns, gas/liquid contact processes and two-phase flow in a duct. However, two-phase flow consists of various levels of mixing of gas and liquid. Two extreme cases are either that gas is a continuous phase or that liquid is a continuous phase. In between these two extreme cases, many different levels of dispersed states exist for both gas and liquid phases. Because of these complicated states, the establishment of mathematical model equations for two-phase flow is quite behind to that for single phase flow problems. In the present report, we treat the system which consists of water as a continuous phase and air bubbles as a dispersed phase. There are many mathematical models proposed even for this simple flow system but we employ the dispersed flow model in this report as follows.

Nomenclature

C_D	= drag coefficient	[-]
C_L	= lift force coefficient	[-]
D_b	= d/r_0	[-]
d	= diameter of a bubble	[m]
g	= acceleration coefficient due to gravity	[m/s^2]
h	= height of liquid surface	[m]
P	= p/p_0	[-]
p	= pressure	[Pa]
p_0	= reference pressure	[Pa]
Q	= injected gas flow rate	[m^3/s]
R	= r/r_0	[-]
r	= radial coordinate	[m]
r_0	= reference length	[m]
r_c	= radius of gas injection hole	[m]
r_{out}	= radius of a tank	[m]
Re	= Reynolds number of a gas bubble	[-]
t	= time	[sec]
t_0	= reference time	[sec]
U	= u/u_0	[-]
u	= radial velocity	[m/s]
u_0	= reference velocity	[m/s]
V	= v/u_0	[-]
v	= vertical velocity	[m/s]
v_r	= slip velocity (= v_g-v_l)	[m/s]
W	= w/u_0	[-]
w	= inlet velocity of gas	[m/s]
Z	= z/r_0	[-]
z	= vertical coodinate	[m]
α_g	= void fraction (gas hold-up)	[-]
μ	= viscosity	[Pa· s]
ν	= kinematic viscosity	[m^2/s]
ρ	= density	[kg/m^3]
ρ^*	= ρ_l / ρ_g	[-]

Subscripts

g	= gas phase
k	= gas phase($k = g$) or liquid phase($k = l$)
l	= liquid phase
r	= r-component

Model System

The system considered is shown in Fig. 1. It is a vertical cylinder whose height is 8 cm and its diameter

Received October 8, 1997
Dedicated to Professor Masashi TASHIRO on the occasion of his retirement
*Interdisciplinary Graduate School of Engineering Sciences, Kyushu Univ.

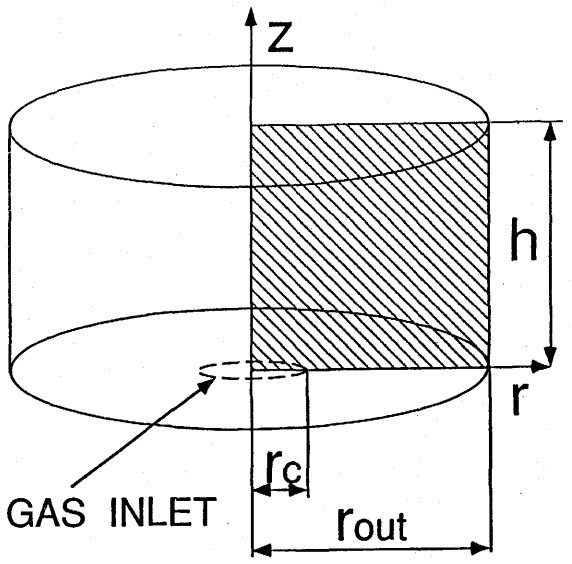

Fig. 1 Schematics of the system of two-phase flow in a vertical water tank. Shaded area is modeled.

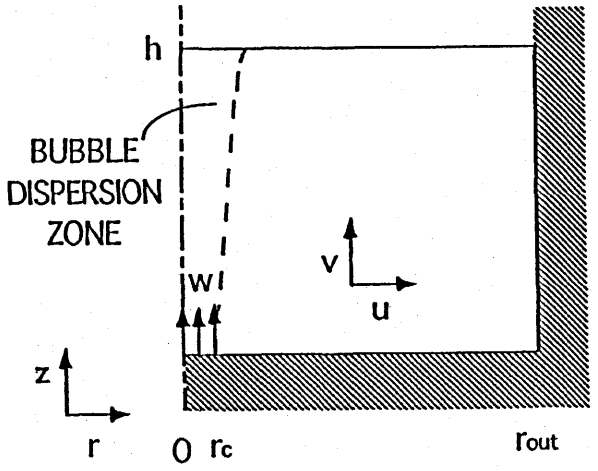

Fig. 2 A vertical side view of the modeled area with coordinates and velocity components.

is 16 cm with a gas inlet hole of 2 cm diameter. Water is filled up of this cylinder and air is injected though a glass filter of 2 cm diameter inlet at a bottom center. Figure 2 shows a vertical side view of this cylinder with a coordinate system and schematics of the bubble dispersed region in the center.

Model equations for two-phase flow are either a one-pressure model (equal pressure both for gas and liquid) or a two-pressure model (different pressure for gas and liquid). The one-pressure model has been known to be mathematically unstable[1] and gives multiple solutions for a single initial condition. However, such defects are also known to be stabilized by viscous forces or virtual mass forces[2]. Two-pressure model is mathematically sound[3] and the dispersed model does not have the pressure gradient term[4].

In the present work, the dispersed model was employed since the dispersed bubbles are not affected by the pressure gradient of separate gas bubbles and this model appears to be mostly sound from physical point of view.

Following assumptions were adopted.

1. There is no phase change between gas and liquid.
2. Densities are constant for both gas and liquid.
3. Flow is axially symmetric two-dimensional in a vertical cylinder.
4. Both gas and liquid are at equal temperature .
5. There is no collision or break-up of bubbles.

The mathematical model equations are as follows in dimensionless variables.

Equation of continuity

$$\left\{\frac{1}{R}\frac{\partial}{\partial R}\left(R\alpha_g U_g\right)+\frac{\partial}{\partial Z}\left(\alpha_g V_g\right)\right\}+\left\{\frac{1}{R}\frac{\partial}{\partial R}\left(R\alpha_\ell U_\ell\right)+\frac{\partial}{\partial Z}\left(\alpha_\ell V_\ell\right)\right\}=0$$

Momentum equation for liquid in the radial direction

$$\begin{aligned}&\frac{\partial U_\ell}{\partial \tau}+U_\ell\frac{\partial U_\ell}{\partial R}+V_\ell\frac{\partial U_\ell}{\partial Z}\\&=-\frac{\partial P}{\partial R}+\left[\frac{2}{R}\frac{\partial}{\partial R}\left(R\frac{\partial U_\ell}{\partial R}\right)+\frac{\partial}{\partial Z}\left\{\left(\frac{\partial V_\ell}{\partial R}+\frac{\partial U_\ell}{\partial Z}\right)\right\}-2\frac{U_\ell}{R^2}\right]\\&\quad+\frac{3}{4}C_D\frac{\alpha_g}{\alpha_\ell}\frac{\left(U_g-U_\ell\right)\left|U_g-U_\ell\right|}{D_b}\\&\quad+C_L\frac{\alpha_g}{\alpha_\ell}\left(V_g-V_\ell\right)\left(\frac{\partial V_\ell}{\partial R}-\frac{\partial U_\ell}{\partial Z}\right)\end{aligned}$$

Momentum equation for liquid in the vertical direction

$$\begin{aligned}&\frac{\partial V_\ell}{\partial \tau}+U_\ell\frac{\partial V_\ell}{\partial R}+V_\ell\frac{\partial V_\ell}{\partial Z}\\&=-\frac{\partial P}{\partial Z}+\left[\frac{1}{R}\frac{\partial}{\partial R}\left\{R\left(\frac{\partial V_\ell}{\partial R}+\frac{\partial U_\ell}{\partial Z}\right)\right\}+2\frac{\partial}{\partial Z}\left(\frac{\partial V_\ell}{\partial Z}\right)\right]\\&\quad+\frac{3}{4}C_D\frac{\alpha_g}{\alpha_\ell}\frac{\left(V_g-V_\ell\right)\left|V_g-V_\ell\right|}{D_b}\\&\quad+C_L\frac{\alpha_g}{\alpha_\ell}\left(U_g-U_\ell\right)\left(\frac{\partial U_\ell}{\partial Z}-\frac{\partial V_\ell}{\partial R}\right)+\left(\frac{1}{\rho^*}-1\right)\end{aligned}$$

Momentum equation for gas in the radial direction

$$\begin{aligned}&\frac{\partial U_g}{\partial \tau}+U_g\frac{\partial U_g}{\partial R}+V_g\frac{\partial U_g}{\partial Z}\\&=-\frac{3}{4}C_D\rho^*\frac{\left(U_g-U_\ell\right)\left|U_g-U_\ell\right|}{D_b}\end{aligned}$$

$$-C_L\rho^*\left(V_g-V_\ell\right)\left(\frac{\partial V_\ell}{\partial R}-\frac{\partial U_\ell}{\partial Z}\right)$$

Momentum equation for liquid in the vertical direction

$$\frac{\partial V_g}{\partial \tau}+U_g\frac{\partial V_g}{\partial R}+V_g\frac{\partial V_g}{\partial Z}$$
$$=-\frac{3}{4}C_D\rho^*\frac{\left(V_g-V_\ell\right)\left|V_g-V_\ell\right|}{D_b}$$
$$-C_L\rho^*\left(U_g-U_\ell\right)\left(\frac{\partial U_\ell}{\partial Z}-\frac{\partial V_\ell}{\partial R}\right)+\left(\rho^*-1\right)$$

In the above equations following values or equations were adopted. Following Drew and Lahey[5], lift force for a single spherical gas bubble was presumed.

$$C_L = 1/2$$

Following Stokes and Schiller Naumann[6],

$$C_D=\begin{cases}24/\mathrm{Re} & at\quad \mathrm{Re}\le 2,\\ 24\dfrac{\left(1+0.15\mathrm{Re}^{0.687}\right)}{\mathrm{Re}} & at\quad \mathrm{Re}>2,\end{cases}$$

where Re is based on a bubble. The above equations are based on the following dimensionless variables.

$R = r/r_0$, $Z = z/r_0$, $D_b = d/r_0$, $U_\ell = u_\ell/u_0$, $V_\ell = v_\ell/u_0$,

$U_g = u_g/u_0$, $V_g = v_g/u_0$, $W = w/u_0$, $\tau = t/t_0$, $P = p/p_0$,

$\rho^* = \rho_\ell/\rho_g$, $r_0 = (\nu_\ell^2/g)^{1/3}$, $u_0 = (g\nu_\ell)^{1/3}$, $t_0 = (\nu_\ell/g^2)^{1/3}$,

$p_0 = \rho_\ell(g\nu_\ell)^{2/3}$.

Initial conditions are as follows.

$$U_\ell = V_\ell = 0$$
$$U_g = V_g = 0$$
$$\alpha_g = 0$$
$$\alpha_\ell = 0$$

Boundary conditions are as follows and these are listed in Fig. 3.

For liquid,

$$U_\ell = 0 \qquad at\quad R=0, R_{out}, Z=0$$
$$\frac{\partial U_\ell}{\partial Z}=0 \qquad at\quad Z=H$$
$$V_\ell = 0 \qquad at\quad R=R_{out}, Z=0, H$$
$$\frac{\partial V_\ell}{\partial R}=0 \qquad at\quad R=0$$

For gas

$$U_g = 0 \qquad at\quad Z=0,\quad R=0, R_{out}$$
$$\frac{\partial U_g}{\partial Z}=0 \qquad at\quad Z=H$$
$$V_g = 0 \qquad at\quad Z=0,\quad R=R_c \sim R_{out}$$
$$V_g = W \qquad at\quad Z=0,\quad R=0 \sim R_c$$
$$\frac{\partial V_g}{\partial R}=0 \qquad at\quad R=0, R_{out}$$
$$\frac{\partial V_g}{\partial Z}=0 \qquad at\quad Z=H$$

For void fraction of gas

$$\alpha_g = 0 \qquad at \qquad Z=0 \qquad \left(R=R_c \sim R_{out}\right)$$
$$\alpha_g = \alpha_{in} \qquad at \qquad Z=0 \qquad \left(R=0 \sim R_c\right)$$
$$\frac{\partial \alpha_g}{\partial R}=0 \qquad at \qquad R=0, R_{out}$$
$$\frac{\partial \alpha_g}{\partial Z}=0 \qquad at \qquad Z=H$$

Above simultaneous partial differential equations were approximated by HSMAC finite difference equations and numerically solved with first order upwind scheme for inertial terms, otherwise second order central difference scheme. The computational region was divided by a staggered grid system as shown in Fig. 4 (a) 24×24 and (b) 96×80 in radial and axial directions.

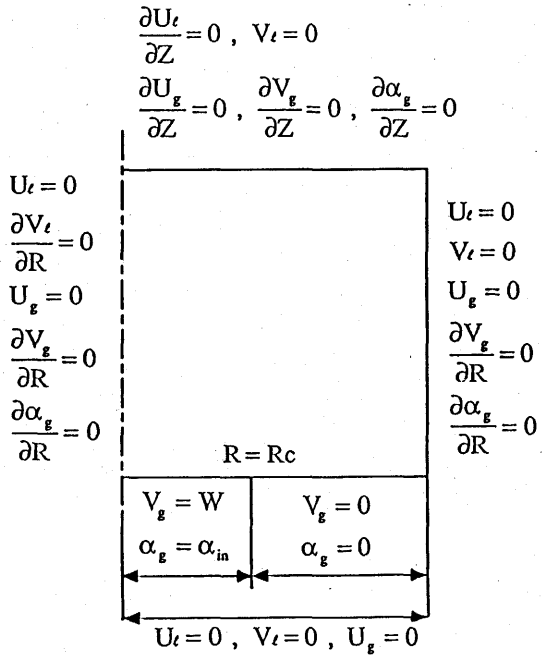

Fig. 3 Summary of the boundary conditions adopted for the right hand side of a vertical cylinder.

Computed Results

Computations were carried out for following conditions. Diameter of bubbles was assumped to be uniform and 1 mm, i. e. , d=1[mm]. Inlet gas flow rate was assumed to be Q = [100 ml/min] with the density ρ_g = 1.161[kg/m^3]. Physical properties of water are as follows.

$\rho_\ell = 998.2$ $[kg/m^3]$

$\mu_\ell = 1.002\times10^{-3}$ $[Pa\cdot s]$

$\nu_\ell = 1\times10^{-6}$ $[m^2/s]$

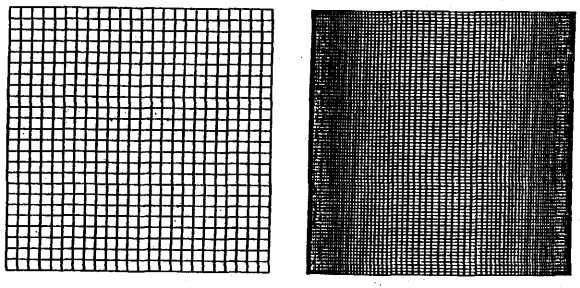

(a) (b)

Fig. 4 Grid allocations.
(a) 24×24, (b) 96×80

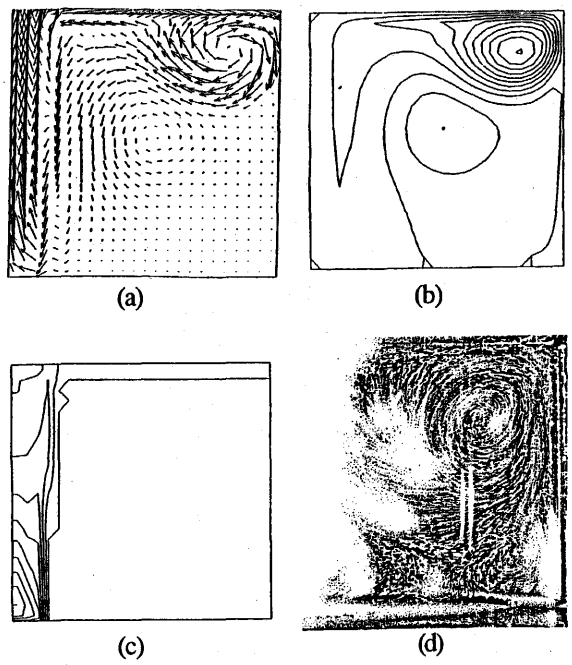

(a) (b) (c) (d)

Fig. 5 Computed result with grid numbers of 24×24.
(a) Liquid velocity vectors
(b) Contours for stream function
(c) Computed profile of void fraction
(d) Visualized vortex with aluminum powder dispersed

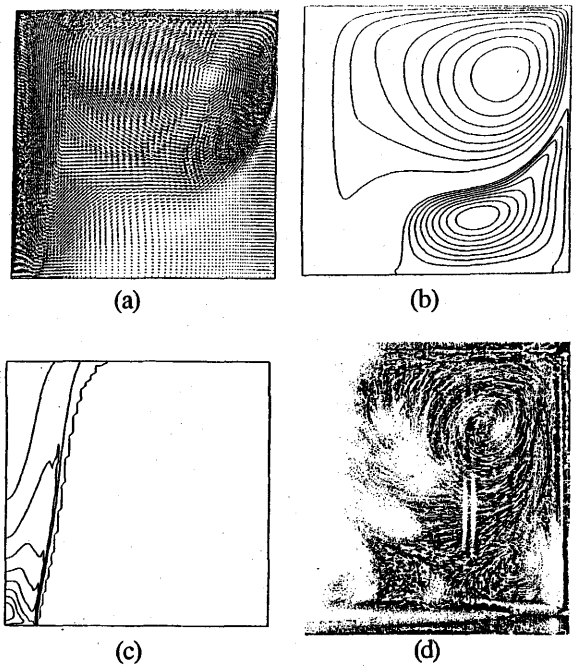

(a) (b) (c) (d)

Fig. 6 Computed result with grid numbers of 96×80.
(a) Liquid velocity vectors
(b) Contours for stream function
(c) Computed profile of void fraction
(d) Visualized vortex with aluminum powder dispersed

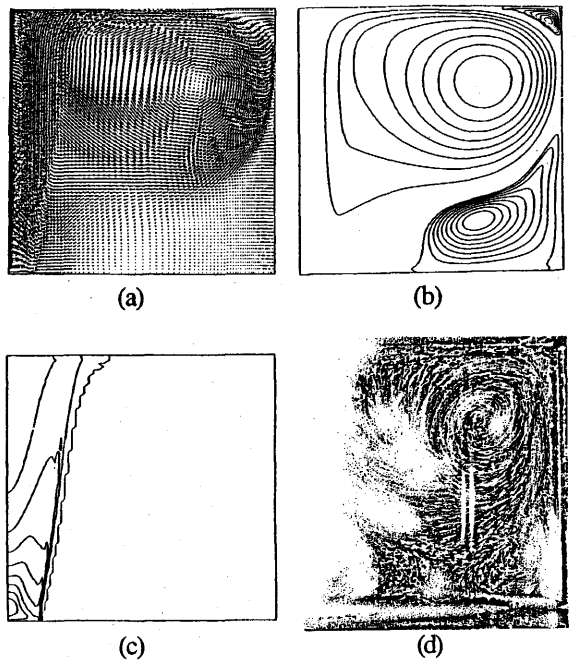

(a) (b) (c) (d)

Fig. 7 Computed result with grid numbers of 96×80 with rigid boundary on the top surface of water layer.
(a) Liquid velocity vectors
(b) Contours for stream function
(c) Computed profile of void fraction
(d) Visualized vortex with aluminum powder dispersed

Figure 5 shows converged result with 24×24 grids for right half region of a cylinder. Figure 5 (a) shows velocity vectors of liquid with the maximum value of 9.99. There is a strong ascending flow due to the buoyancy for bubbles along the axis of a cylinder(left hand side of picture (a)). Figure 5 (b) shows contour maps of stream function to represent steady state streak line with the value between -9.18×10^5 to 1.74×10^5. There is a strong circulation vortex near the top and right hand side of a cylinder. Figure 5 (c) shows contour maps of void fraction computed. Bubbles are dense near the central bottom area. Figure 5 (d) shows corresponding flow visualization picture with aluminum powder dispersed. General flow modes are in agreement between computed contours of stream function and the photograph but not enough on the detailed shape and locations of the vortex.

Figure 6 shows corresponding results with radial and vertical grid numbers of 96×80. Magnitude and location of a vortex in Figs. 6 (a) and (b) agree quite well with the experimental picture, Fig. 6 (d).

These two results of Figs. 5 and 6 are for free slip condition on the water surface. Further computation was carried out for rigid condition on the water surface as shown in Fig. 7. Even a small vortex on the upper right hand corner could have been simulated which is similar to the photograph. This means that the boundary condition of rigid wall is better than free slip condition.

Conclusion

Two-dimensional dispersed flow model in a vertical cylinder was derived and numerically computed with both coarse and minute grid sizes. The results with minute grid sizes and with the rigid top surface for water gave quite reasonable solutions for the size and location of a vortex in water in comparison with the experimental result.

References

1. Lyczkowski, R.W., Solbring, C. W., Gidaspaw D. and Hughes, E. D. ; Nucl. Sci. Eng., **66**, (1978) 378-396.
2. Nihon Genshiryoku Gakkai, Numerical Analyses of Two phase flow, Asakura (1993).
3. Ransom, V. H. and Hicks, D. L., ; J. Comp. Phys., **5 3**, (1984) 124-151.
4. Kataoka, I. and Tomiyama, A. ; Japanese J. Multiphase Flow, **7**, (1993) 132-141.
5. Drew, D. A. and Lahey, R. T. ; Int. J. Multiphase Flow, **5**, (1979) 243-264.
6. Funtaikogaku Binran, Nikkan Kogyo (1986).